Journal of Materials Chemistry C

Accepted Manuscript

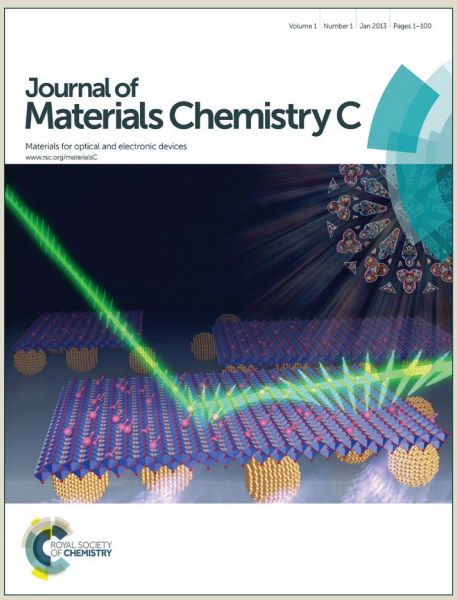

ROYAL SOCIETY OF CHEMISTRY

www.rsc.org/materialsC

Tunable white light emission of Eu, Tb, Zn-Containing Copolymers by RAFT polymerization

Naiqun Sun[a,b], Liping Li[a,b], Yamin Yang[a,b], Xijin Zhao[a,b], Aiqin Zhang[a,c*], Husheng Jia[a,b*], Xuguang Liu[a,d], Bingshe Xu[a,c]

[a] *Key Laboratory of Interface Science and Engineering in Advanced Materials of Taiyuan University of Technology, Ministry of Education, Taiyuan 030024, China;*

[b] *College of Materials Science and Engineering, Taiyuan University of Technology, Taiyuan 030024, China;*

[c] *Research Center of Advanced Materials Science and Technology, Taiyuan University of Technology, Taiyuan, 030024, China;*

[d] *College of Chemistry and Chemical Engineering, Taiyuan University of Technology, Taiyuan, 030024, China;*

[*]**Author to whom correspondence should be addressed.**

E-mails: jia_husheng@126.com; zaq6014567@126.com.

Tel.: +86-351-6010311; Fax: +86-351-6010311; No.79 Yingze Street, Taiyuan, Shanxi

Abstract

In this work, a novel copolymer PS-Eu-Tb-Zn, which can match 365 nm UV chip, was synthesized by RAFT polymerization of Tb(p-BBA)$_3$UA, Eu(TTA)$_2$(Phen)MAA, Zn(BTZ)UA and styrene. TG–DTG and PL analyses indicate that copolymer PS-Eu-Tb-Zn displays favorable thermal stability and luminescent properties. Excited at 365 nm, the copolymer exhibits emission peaks at 421 nm (blue emission), 488, 543 nm (green emission), 589 and 615 nm (red emission). The white light of the copolymer can be obtained by tuning the ratios of three complexes and excitation wavelengths. The CIE coordinates (0.352, 0.330) of the copolymer is optimal upon excitation at 365 nm. For the fabricated white LED using 365 nm UV chip with the copolymer, the CCT is 5684 K, and the CRI is 83.1. All the results indicate that the copolymer can be applied as a phosphor for fabrication of NUV-based white LED.

1. Introduction

With respect to conventional incandescent and fluorescent lamps, white-light emitting diodes (WLEDs) have attracted considerable interest in recent years because of the advantages of high efficiency, low energy consumption, long lifetime and environmental friendliness.[1–6] Presently, the commercially dominant white LEDs are the phosphor-converted white LEDs, in which the "blue chip + yellow phosphor" mode as a convenient way has the defects of low luminous efficiency and low color-rendering index owing to the scarcity of red emission in the visible spectrum.[7] As expected, the "ultraviolet chip + red/green/blue tricolor phosphors" mode can overcome the above drawbacks and improve the light color stability. To a certain degree, the brightness of white light hinges on green light in the "ultraviolet chip + red/green/blue tricolor phosphors" mode, while red and blue light play a role in adjusting color coordinate and color temperature.[8–12] Nonetheless, common green phosphors for white LEDs reported in the research literature have some disadvantages, including low stability for sulfide phosphors and low temperature quenching for silicate phosphors.[13] Therefore, it is an urgent task to find new green phosphors with higher luminescent stability that can be efficiently excited by near UV chip for white LEDs.

Rare earth organic complexes as phosphors provide a new path for fabrication of NUV-based white LEDs, for their stable narrow emission and high luminous efficiency.[14–16] Recently, the researches on terbium complexes with aromatic carboxylic acid are arousing wide concern, since the compounds perform excellent green emission properties and high luminescent stability.[17] However, the majority of terbium complexes with aromatic carboxylic acid has difficulty in matching 365 nm UV chip. For instance, Zheng et al. prepared terbium complex containing trimesic acid with optimal excitation wavelength at 255 nm.[18] Wu et al. reported terbium complex of 6-methyl-2-(3-ethoxycarbonylpyrazol-1-yl)pyridine with the optimal excitation wavelength at 301 nm.[19] Guo and coworkers prepared terbium complex containing benzoic acid with excitation band between 250~360 nm.[20] These terbium complexes demand further improvement to meet excitation by 365 nm UV chip.

In recent years, europium(III) organic complexes as red phosphor[21–24] in the fabrication of white LEDs have been reported because of their wide excitation band, high internal quantum yield, and good color purity.[25–27] Particularly, most studies are focused on zinc(II) complexes to obtain blue light,[28,29] since they are capable of replacing beryllium(II) complexes that could be of harm to

the environment.

Compared with physical blending, which often results in unavoidable bad dispersion and quenching, polymerization is in the limelight to obtain white light. Besides the advantage of the desired mechanical flexibility, rare earth luminescent polymers show excellent electroluminescence and processability in solution or fused state, which are more attractive for optical and electronic applications.[30,31] Presently, reversible addition-fragmentation chain transfer (RAFT)[32,33] polymerization has evolved into a versatile process owing to its compatibility with a large range of functional groups, such as acid and amide. Polymers with narrow molar mass dispersity and controlled molecular weight were gained via RAFT polymerization.[34] Employment of this technique for the synthetic polymers intended for potential applications in optical, biomedical and pharmaceutical technologies has been reported.[35,36]

In this paper, a novel Tb(III) complex $Tb(p\text{-}BBA)_3UA$ that can match 365 nm UV chip was synthesized, meanwhile the red and blue complex monomers $Eu(TTA)_2(Phen)MAA$ and Zn(BTZ)UA were synthesized by covalently bonding metal ions and organic ligands. Subsequently, the copolymer PS-Eu-Tb-Zn was synthesized through RAFT polymerization of the three monomers with styrene. This copolymer has not yet been reported in the literature to the best of our knowledge. The luminescent properties and thermal stability of the copolymer PS-Eu-Tb-Zn were studied in detail. By tuning the ratios of the three complexes and excitation wavelengths, the CIE coordinates of copolymers PS-Eu-Tb-Zn were found to be located in white light region. In addition, the LED device using the copolymer PS-Eu-Tb-Zn as phosphor with a NUV (365 nm) chip was fabricated to demonstrate its applicability as a luminescent material.

2 Experimental

2.1 Materials

$EuCl_3$ and $TbCl_3$ were purchased from Shanghai Diyang Company Limited. $ZnCl_2$, 2-thenoyltrifluoroacetone (TTA), 1,10-phenanthroline (Phen), 2-(2-hydroxyphenyl)benzothiazole (BTZ), 4-benzoylbenzoic acid (p-BBA), methacrylate acid (MAA), undecylenic acid (UA) and 2-methyl-2-[(dodecylsulfanylthiocarbonyl)sulfanyl]propanoic acid (TTCA) were obtained from Alfa Aesar and used as analytical reagent. 2,2-Azoisobutyronitrile (AIBN) was recrystallized twice from methanol. All solvents were obtained in analytical grade from Shanghai Chemical Reagent Company and used as received without further purification.

2.2 Apparatus

Elemental analysis of the complexes was conducted on a Perkin–Elemer Elemental Analyzer. ^{1}H NMR spectra were recorded on a Varian INOVA500NB. FT-IR spectra were recorded using a NICOLET AVATAR 330 Fourier transform infrared (FTIR) spectrometer (KBr pellet, 4000~400cm^{-1}). UV-vis absorption spectrum was taken using a Cary-300 VARIAN spectrometer. Fluorescence spectra and quantum yield were measured by a RF-5301PC Spectro fluorophotometer (slit width was 1 nm). Thermogravimetric analysis was conducted using SDT 2960 Analyzer with the heating rate of 10℃/min under N_2. DSC measurements were performed with a NETZSCH DSC200F3 at a heating rate of 10ºC/min in argon atmosphere. EL spectra were measured with a computer controlled PR655 Spectra scan spectrometer. All measurements were made at room temperature unless otherwise stated.

2.3 Synthesis of complexes **1–3** [Eu(TTA)$_2$(Phen)MAA, Tb(p-BBA)$_3$UA, Zn(BTZ)UA]

Eu(TTA)$_2$(Phen)MAA (complex **1**): Eu(TTA)$_2$(Phen)MAA complex was prepared by a method analogous to our earlier work.[37] One millimole of $EuCl_3$ in 10 mL of ethanol solution and 1 mmol of MAA was mixed under stirring. The pH of the solution was neutralized to 4~5 with 1.0 mol/L sodium hydroxide ethanol solution. Subsequently, 2 mmol of TTA in 5 mL of ethanol was added into the mixed solution. Finally, 1 mmol of Phen in 5 mL of ethanol was dropped and precipitation was observed by adding 1.0 mol/L sodium hydroxide ethanol solution with the pH of the solution among 6.5~7. The solution was refluxed under stirring at 55ºC for 3 h. The precipitate was collected, repeatedly washed with ethanol and dried in vacuum at 90℃ for 24 h. Eu(TTA)$_2$(Phen)MAA: ^{1}H NMR (300 M, $CDCl_3$) δ [ppm]: 1.71 (s, 3H), 2.04 (d, 4H), 5.02 (s, 2H), 6.74–7.05 (d, 6H), 7.32 (s, 2H), 7.63 (s, 2H), 8.02 (s, 2H), 8.78 (s, 2H); elemental analysis for Eu(TTA)$_2$(Phen)MAA is as follows: element analytical (calc.) C 43.92% (43.94%)，H 2.73% (2.74%)，N 3.22% (3.21%)，S 7.34% (7.32%). Yield: 71.95%.

Tb(p-BBA)$_3$UA (complex **2**): The solutions of 3 mmol of 4-BBA in 5 mL of ethanol and 1 mmol of UA in 5 mL of ethanol were mixed. The solution of 1 mmol of $TbCl_3$ in 5 mL of ethanol was added dropwise into the mixed solution while heated and refluxed under stirring at 55 ℃ for 2.5 h. The pH of the solution was controlled to 6~7 by adding 1.0 mol/L sodium hydroxide ethanol solution and precipitate appeared. Finally, the precipitate Tb(p-BBA)$_3$UA was obtained by filtration, washing with anhydrous ethanol and drying in vacuum at 90℃ for 24 h. Tb(p-BBA)$_3$UA:

^{1}H NMR (300 M, $CDCl_3$) δ [ppm]: 1.81–2.35(m, 16H), 4.97–5.21(d, 3H), 7.16 (s, 3H), 7.49 (s, 6H), 7.61 (s, 6H), 7.82 (s, 6H), 8.21 (s, 6H); elemental analysis for Tb(p-BBA)$_3$UA is as follows: element analytical (calc.) C 62.17% (62.54%), H 4.98% (4.52%). Yield: 61.72%.

Zn(BTZ)UA (complex **3**): The pH of 15 mL of ethanol solution containing 1 mmol of $ZnCl_2$, 1 mmol of BTZ and 1 mmol of MAA was neutralized to 7~8 with 1.0 mol/L sodium hydroxide ethanol solution and precipitate appeared. The mixed solution was refluxed under stirring at 55ºC for 4 h. Finally, the precipitate Zn(BTZ)UA was obtained by filtration, washing with ethanol and drying in vacuum at 90℃ for 24 h. Zn(BTZ)UA: ^{1}H NMR (300 M, $CDCl_3$) δ [ppm]: 1.29–1.33(m, 10H), 1.62 (s, 2H),1.96 (s, 2H), 2.23 (s, 2H), 3.2 (s, H), 4.06 (s, H), 5.01 (s, 2H), 5.7(s, H), 5.81–5.9(d, 4H), 6.76–6.85 (d, 2H), 7.11 (d, H), 7.45 (s, H); elemental analysis for Zn(BTZ)UA is as follows: element analytical (calc.) C 60.49% (60.52%), H 6.6% (6.61%), N 2.31% (2.29%), S 6.75% (6.72%). Yield: 69.43%.

The synthesis routes of the complexes **1–3** are depicted as scheme1.

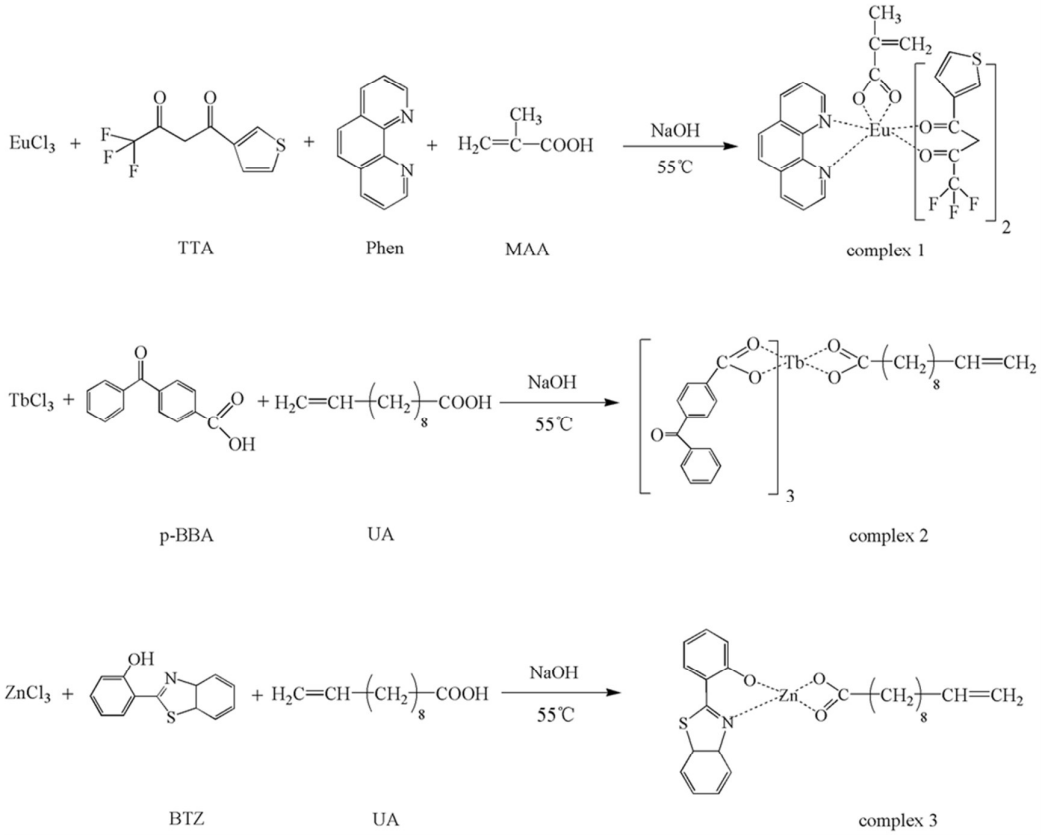

Scheme 1 Synthesis routes of the complexes **1–3**.

2.4 Synthesis of macro-RAFT agent (PS-Eu) with

2-methyl-2-[(dodecylsulfanylthiocarbonyl)sulfanyl]propanoic acid

The following procedure is typical in reported reference.[38,39] The DMSO solution (1.2 mL) containing $Eu(TTA)_2(Phen)MAA$ (44 mg), 2-methyl-2-[(dodecylsulfanylthiocarbonyl)sulfanyl]propanoic acid (TTCA, 13.2 mg), AIBN (1.23 mg), and styrene (0.86 mL) was transferred to an ampoule, was degassed by three freeze-evacuate-thaw cycles, sealed and then heated at 70 °C. The macro-RAFT PS-Eu-TTCA was precipitated into methanol and collected by centrifugation. The purification of PS-Eu was carried out with repeated dissolution in DMF and precipitation from methanol. PS-Eu was finally washed with methanol and dried under vacuum at 55 °C for 12 h. FT-IR spectrum of (PS-Eu) [cm^{-1}]: 3028 (ν C–H); 2924 (ν $–CH_2$); 1721 (ν C=O); 1451–1494 (ν C=C, ν C=N); 1281 (ν $–CF_3$); 701 (ν C–H); 442 (ν Eu–O). GPC: M_n (g/mol) 5238, M_w (g/mol) 6706, PDI 1.16.

2.5 Synthesis of block copolymer (PS-Eu)-*b*-(PS-Tb)

The DMSO solution (1.2 mL) containing $Tb(p\text{-}BBA)_3UA$ (254 mg), (PS-Eu) (M_n 5238, 392.9 mg, 0.075 mmol), AIBN (1.23 mg), and styrene (0.86 mL) was transferred to an ampoule, was degassed by three freeze-evacuate-thaw cycles, sealed and then heated at 70 °C. The macro-RAFT PS-Eu-Tb-TTCA was precipitated into methanol and purified by repeating dissolution in DMF and precipitation from methanol. Finally, (PS-Eu)-*b*-(PS-Tb) was washed with methanol and dried under vacuum at 55 °C for 12 h. FT-IR spectrum of (PS-Eu)-*b*-(PS-Tb) [cm^{-1}]: 3028 (ν C–H); 2924 (ν $–CH_2$); 1724 (ν C=O); 1451–1493 (ν C=C, ν C=N); 1281 (ν$–CF_3$); 699 (ν C–H); 443 (ν Eu–O); 420 (ν Tb–O). GPC: M_n (g/mol) 10217, M_w (g/mol) 12669, PDI 1.24.

2.6 Synthesis of block copolymer (PS-Eu)-*b*-(PS-Tb)-*b*-(PS-Zn) [PS-Eu-Tb-Zn]

The DMSO solution (1.2 mL) containing Zn(BTZ)UA (8.8 mg), (PS-Eu)-*b*-(PS-Tb) (M_n 10217, 766.3 mg, 0.075 mmol), AIBN (1.23 mg), and styrene (0.86 mL) was transferred to an ampoule, was degassed by three freeze-evacuate-thaw cycles, sealed and then heated at 70 °C. The block copolymer PS-Eu-Tb-Zn was precipitated into methanol and purified by repeating dissolution in DMF and precipitation from methanol. Finally, the block copolymer was washed with methanol and dried under vacuum at 55 °C for 12 h. FT-IR spectrum of (PS-Eu)-*b*-(PS-Tb)-*b*-(PS-Zn) [cm^{-1}]: 3028 (ν C–H); 2924 (ν $–CH_2$); 1724 (ν C=O); 1451–1493 (ν C=C, ν C=N); 1281 (ν $–CF_3$); 699 (ν C–H); 486 (ν Zn–O); 443 (ν Eu–O); 420 (ν Tb–O). GPC: M_n 14983 (g/mol), M_w (g/mol) 19927, PDI 1.33.

The synthesis routes of the copolymer (PS-Eu)-*b*-(PS-Tb)-*b*-(PS-Zn) are depicted as scheme 2.

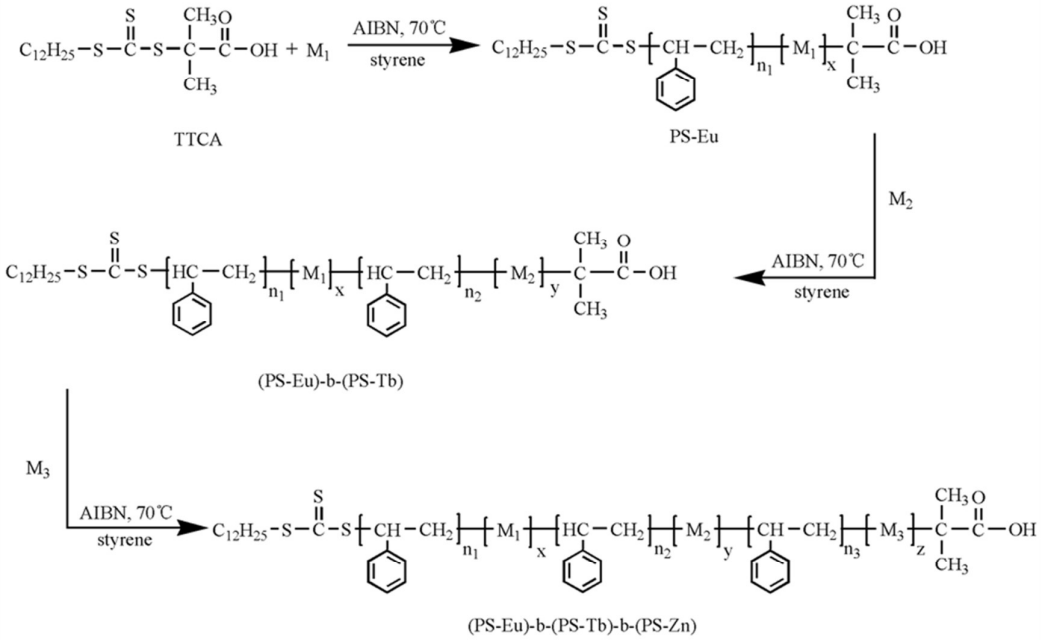

Scheme 2 Synthesis routes of the copolymer (PS-Eu)-*b*-(PS-Tb)-*b*-(PS-Zn), M_1=complex **1**, M_2=complex **2**, M_3=complex **3**.

2.7 Synthesis of copolymers **1–8**

Copolymers **1–8** are the copolymer PS-Eu-Tb-Zn with different ratios of Eu(III), Tb(III) and Zn(II) complexes (complexes **1–3**). Copolymers **1–8** were synthesized in accordance with the synthesis method of PS-Eu-Tb-Zn. The main parameters of copolymers **1–8** are listed in Table 1.

Table 1 Molecular weight, conversion and the ratio of Eu(III),Tb(III) and Zn(II) complexes (complexes **1–3**) for copolymers **1–8**

Copolymer	Eu(III)/Tb(III) /Zn(II) complex	[St]/[RAFT agent] /[AIBN]	Conversion (%)	$M_{n\ (GPC)}$ (g/mol)	PDI
1	1: 6: 3.3	200: 1: 0.2	28.4	14992	1.34
2	1: 6.5: 0.6	200: 1: 0.2	29.2	15017	1.36
3	1: 10: 1.2	200: 1: 0.2	30.3	15521	1.38
4	1: 5: 0.4	200: 1: 0.2	28.1	14983	1.33
5	1: 6: 0.45	200: 1: 0.2	28.8	15046	1.36
6	1: 2.2: 0.4	200: 1: 0.2	27.8	15821	1.41
7	1: 6.5: 0.25	200: 1: 0.2	29.3	15033	1.37
8	1: 2.5: 0.2	200: 1: 0.2	27.4	15751	1.40

3 Results and discussion

3.1 IR spectra

The IR spectra of copolymer PS-Eu-Tb-Zn and homopolymer PS are given in Fig.1. The C–H stretching vibration and $–CH_2$ stretching vibration of PS occur at 3028 and 2924 cm^{-1}, the C=C stretching vibration of PS at 1492 cm^{-1} is well identified in PS-Eu-Tb-Zn. The IR spectra of copolymer PS-Eu-Tb-Zn are extremely similar to those of homopolymer PS, which may be due to the very low content of complexes in the copolymer.[40] Nonetheless, there are some subtle differences between copolymer PS-Eu-Tb-Zn and homopolymer PS. The characteristic bands in PS-Eu-Tb-Zn at 1724 and 1282 cm^{-1} are assigned to the stretching vibration of C=O in complex **2** and the stretching vibration of $–CF_3$ in complex **1**, respectively. Besides, the weak characteristic bands in PS-Eu-Tb-Zn at 486, 443 and 420 cm^{-1} are attributed to the stretching vibration of Zn–O in complex **3**, Eu–O in complex **1** and Tb–O in complex **2**, respectively. All these results imply that complexes **1–3** are organized into polymer chain by copolymerization.

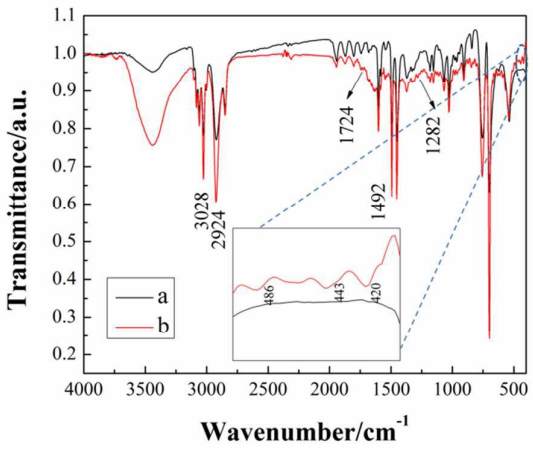

Fig. 1 IR spectra of homopolymer PS (a) and copolymer PS-Eu-Tb-Zn (b) in solid state.

3.2 UV–Visible absorption spectra

The UV–vis absorption spectra of complexes **1–3** and copolymer PS-Eu-Tb-Zn in DMF solution (1×10^{-4} mol/L) are displayed in Fig. 2. The absorption band for copolymer PS-Eu-Tb-Zn at 263–311 nm is primarily attributed to the joint effect of the n-π^* transition of C=N[41] in complex **1** and π–π* transition of conjugate structure between benzene ring with carboxyl and carbonyl in complex **2**. Moreover, the absorption band for copolymer PS-Eu-Tb-Zn at 311–368 nm is mainly ascribed to the n–π* transition of nonbonding lone pair electrons in carbonyl and thiophene in complex **1**. Further, the weak absorption band for copolymer PS-Eu-Tb-Zn at 368–420 nm is

assigned to the intramolecular charge transition from phenol ring to benzothiazole in complex **3**.[42] These results further indicate that complexes **1–3** are polymerized into polymer chain.

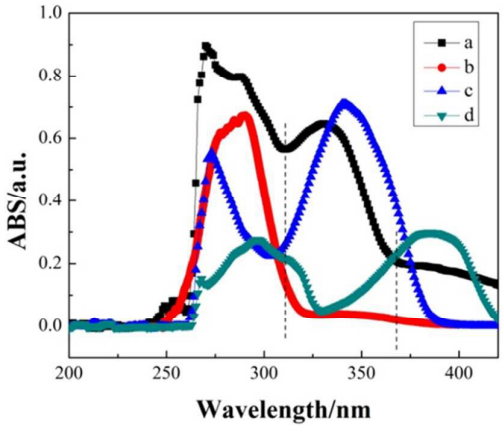

Fig. 2 UV-vis absorption spectra of copolymer PS-Eu-Tb-Zn (a), complex **2** (b), complex **1** (c) and complex **3** (d).

3.3 Thermal properties

The thermal properties of copolymer PS-Eu-Tb-Zn were investigated by differential scanning calorimetry (DSC) measured under argon atmosphere, thermogravimetric (TG) analysis and differential thermal gravimetric (DTG) analysis measured under nitrogen atmosphere. As is seen from Fig. 3 (a), the glass transition temperature (T_g) of copolymer is 31℃ higher than that of PS (105℃). This result indicates that T_g of copolymer can be enhanced upon the introduction of the complex moieties into the polymer chain.[43] Since the complexes have some rigid groups, the chain flexibility of polymer chain is lowered. Besides, the complexes are quite bulky, the mobility of the polymer chain is restricted as a result of the steric hindrance, leading to an increased T_g value.[44–46] It is obvious that copolymer PS-Eu-Tb-Zn remains stable up to 307℃ (Fig. 3 (b)). In particular, the weight loss of copolymer at around 307℃ is primarily attributed to the removal of ligands from the complexes. The maximum decomposition rate of copolymer occurs at 408℃, which is assigned to the decomposition of main chain of polymer. In view of operation temperature of LED below 150℃,[47,48] copolymer PS-Eu-Tb-Zn is thermally stable enough for fabrication of LED.

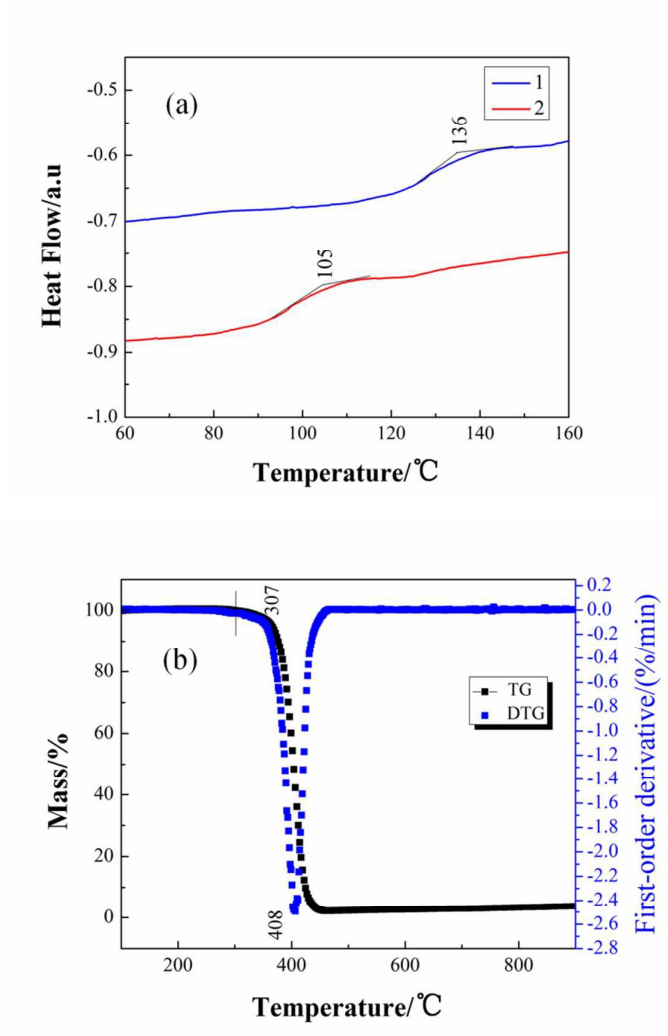

Fig. 3 (a) DSC curves of copolymer PS-Eu-Tb-Zn (1) and PS (2), (b) TG–DTG curves of copolymer PS-Eu-Tb-Zn.

3.4 Photoluminescence properties

The solid-state excitation and emission spectra of complexes **1–3** recorded at room temperature are displayed in Fig. 4. Complex **1** shows pure red emission at 612 nm due to $^5D_0 \rightarrow {}^7F_2$ transition, and complex **2** exhibits pure green emission at 543 nm due to $^5D_4 \rightarrow {}^7F_5$ transition. Complex **1** exhibits emission peaks at 578, 590, 612 and 651 nm related to $^5D_0 \rightarrow {}^7F_J$ transitions of Eu^{3+}, where J=0–3, respectively, when excited at 365 nm.[49,50] On the other hand, complex **2** displays typical emission bands at 488, 543, 584 and 619 nm, corresponding to transitions from $^5D_4 \rightarrow {}^7F_J$ (where J=6–3, respectively) of Tb^{3+} (λ_{ex}=365 nm).[51,52] Complex **3** shows blue emission at 452 nm when excited at 365 nm. It is obvious from Fig. 4 that complexes **1–3** can well match 365 nm UV chip.

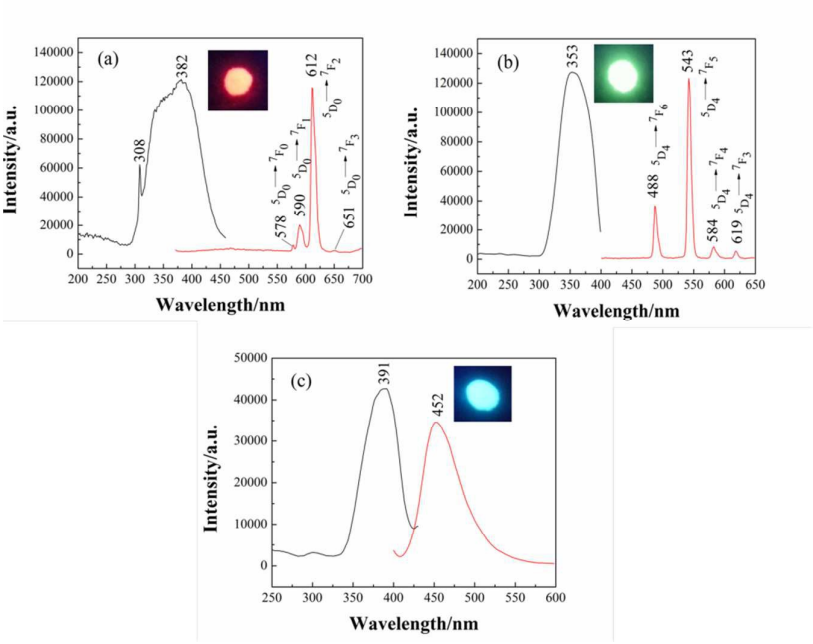

Fig. 4 Room-temperature excitation and emission spectra of complex **1** (a), complex **2** (b) and complex **3** (c) excited at 365 nm.

Fig. 5 displays the emission peaks of copolymer **5** at 421 nm (blue emission of complex **3**), 488, 543 nm (green emission of complex **2**), 589 and 615 nm (red emission of complex **1**). There is little, if any, change in green and red emission in copolymer **5** with respect to that in complex **2** and complex **1**, since the 4f electrons of Eu^{3+} and Tb^{3+} are shielded by 5s5p electrons and the characteristic peaks of Eu^{3+} and Tb^{3+} are insensitive to environment.[53] Nonetheless, the blue shift (31 nm) of blue emission in copolymer **5** is observed compared with complex **3**. Actually, luminescent mechanism of complex **3** is fully different from that of complexes **1** and **2**. The photoluminescence of complex **3** is attributable to ligand-based π–π* transition.[54,55] In the energy level transition, the absorbed energy of polymer chain is partially passed to ligand BTZ, resulting in the decrease of energy loss of the nonradiative transition. Thus, the blue emission is blue shifted to 421 nm in copolymer **5**.

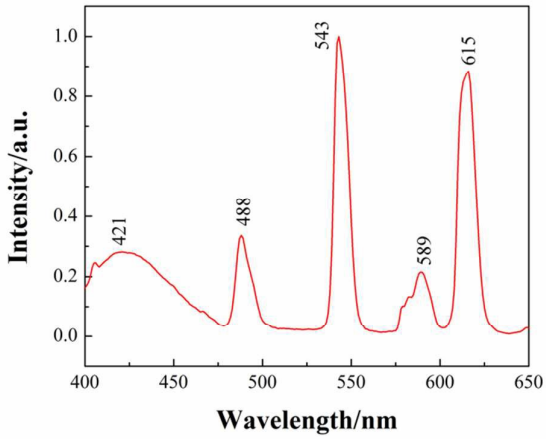

Fig. 5 The emission spectrum of copolymer **5** excited at 365 nm.

The emission profiles of copolymers **1–8** excited at 365 nm are shown in Fig. 6 and the corresponding CIE chromaticity coordinates are marked in Fig. 7. Copolymers **1–8** exhibit mixed emission patterns with different relative peak intensities resting with the ratios of complexes **1–3**, leading to a fluent change of their visible photoluminescence emission colors among red, green and blue. With the adjustment of the ratios of complexes **1–3**, a variety of colors around the white light zone are obtained, such as wathet blue, reseda, light pink and pale yellow. In particular, a series of coordinates of white light zone (copolymers **2, 4, 5** and **7** in Fig. 6) are achieved by tuning the ratios of complexes **1–3**. Among the coordinates of white light region, (0.352, 0.330) of copolymer **5** is highly close to pure white light (0.330, 0.330) according to the 1931 CIE coordinate diagram.[56–58]

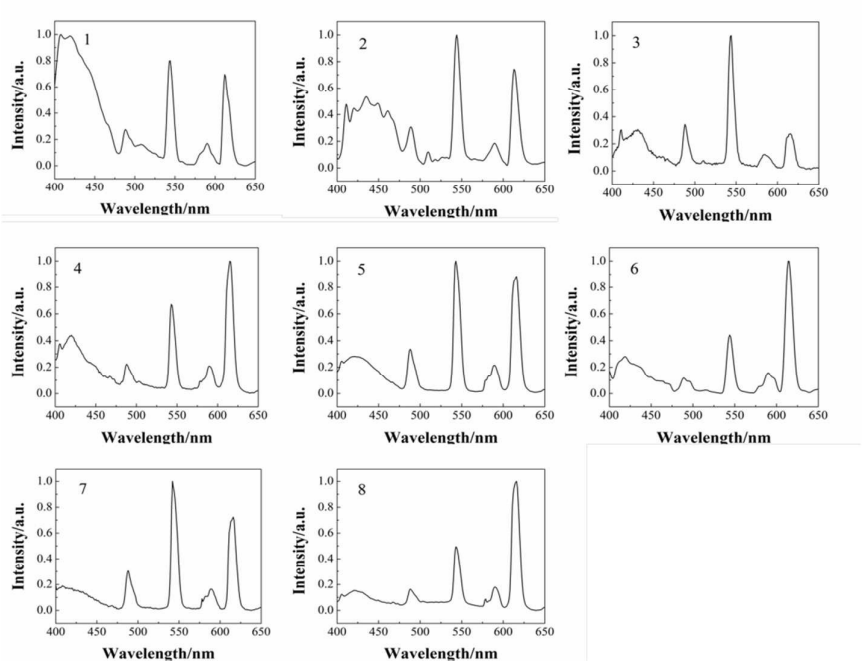

Fig. 6 The emission spectra of copolymers **1–8** excited at 365 nm.

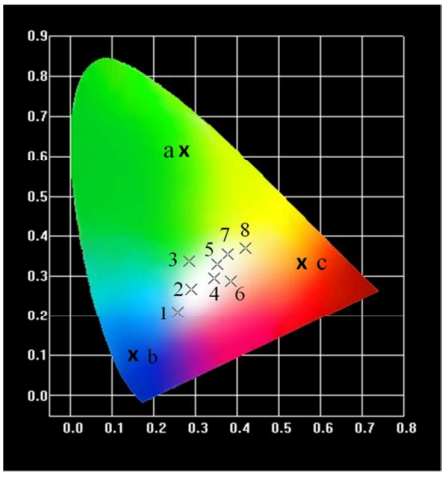

Fig. 7 The CIE chromaticity coordinates for complexes **1–3** (a–c) and copolymers **1–8** excited at 365 nm [a:(0.275, 0.611), b:(0.145, 0.103), c:(0.546, 0.332),1: (0.258, 0.211), 2: (0.289, 0.267), 3: (0.286, 0.338), 4: (0.344, 0.294), 5: (0.352, 0.330), 6: (0.386, 0.287), 7: (0.377, 0.354), 8: (0.421, 0.371)].

The emission behavior of copolymer **7** investigated by varying the excitation wavelengths between 360 and 380 nm is displayed in Fig. 8 and the corresponding CIE chromaticity coordinates are shown in Fig. 9. It is obvious that along with the change of excitation wavelength from 360 to 380 nm, the characteristic peak at 543 nm (green emission) becomes lower, while those at 615 nm (red emission) and 420–450 nm (blue emission) become stronger. This change can be ascribed to the change in the match degree between the excitation bands of complexes **1–3** and the excitation wavelength.[59,60] The optimal excitation wavelength of complex **2** is 353 nm and

the intensity of excitation bands is reduced with the excitation wavelength changing from 360 to 380 nm. In turn, the match degree between the excitation bands of complexes **1** and **3** and the excitation wavelength becomes better with the excitation wavelength changing from 360 to 380 nm. Therefore, the y value of corresponding CIE chromaticity coordinates of copolymer **7** is decreased when the excitation wavelength varies from 360 to 380 nm and the component of green emssion is declined. Accordingly, with the increase in excitation wavelength, the CIE coordinates vary from light yellow emission (0.383, 0.394) excited at 360 nm to white emission (0.349, 0.278) upon excitation at 380 nm. The CIE chromaticity coordinates of copolymer **7** are found to be (0.351, 0.330) excited at 370 nm, which is very close to pure white light (0.330, 0.330) according to the 1931 CIE coordinate diagram.

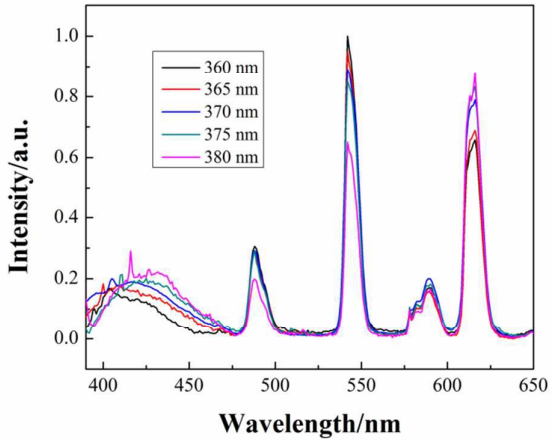

Fig. 8 The emission spectra of copolymer **7** under the excitation wavelengths of 360–380 nm.

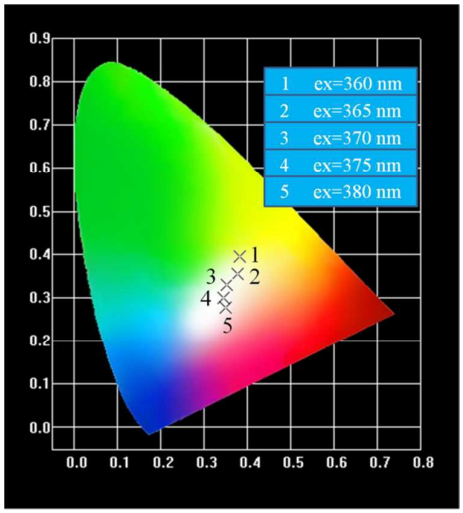

Fig. 9 The CIE chromaticity coordinates for copolymer **7** under the excitation wavelengths of 360–380 nm [360 nm: (0.383, 0.394), 365 nm: (0.377, 0.354), 370 nm: (0.351, 0.330), 375 nm:

(0.345, 0.301), 380 nm: (0.349, 0.278)].

The overall quantum yield (φ_S) of copolymer PS-Eu-Tb-Zn was also measured in 10^{-3} mol/L DMF by using $Eu(TTA)_3phen$ as a reference: $\varphi_S=\varphi_R A_R I_S N_S^2/A_S I_R N_R^2$, where φ_R=0.365 is the quantum yield of $Eu(TTA)_3phen$ in 10^{-3} mol/L DMF,[61] n, A, and I refer to the refractive index of solvent, the area of the emission spectrum, and the absorbance intensity at the excitation wavelength, respectively. The overall quantum yield (φ_S) of copolymer PS-Eu-Tb-Zn is 0.17, indicating that the copolymer phosphor is a promising luminescent material.

3.5 WLED fabricated with copolymer **5** as phosphor

In order to further demonstrate the potential application of copolymer PS-Eu-Tb-Zn, copolymer **5** was used to realize the white light by using NUV LED chip (365 nm). Fig. 10 displays the electroluminescence (EL) spectrum of the fabricated WLED with the phosphor copolymer **5** driven at 3.8 V, and practical emission of the fabricated WLED in inset photographs. EL spectrum of the fabricated WLED exhibits blue, green and red emissions, which are admirably consistent with those of phosphor copolymer **5**. Besides, the CIE chromaticity coordinates corresponding to the electroluminescence of the fabricated WLED (0.354, 0.337) and the photoluminescence of phosphor copolymer **5** (0.352, 0.330) are greatly similar. The results imply that when used to fabricate WLED, phosphor copolymer **5** still maintains qualified luminescent performance. Moreover, the optical properties of the fabricated WLED also show that the CCT is 5684 K, the CRI (R_a) is 83.1. In comparison with the WLED based on blue InGaN chip and $YAG:Ce^{3+}$ phosphor (R_a=75, CCT=7756 K),[62,63] the WLED in this study shows higher R_a value and lower CCT value, indicating copolymer **5** can be a promising candidate for application in NUV-based white LED.

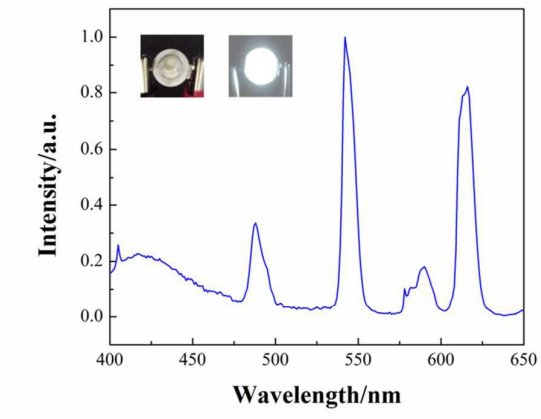

Fig. 10 Electroluminescence (EL) spectrum of the fabricated WLED with the phosphor copolymer **5** at 3.8 V. The inset photographs are the WLED lamp package.

4. Conclusions

A novel copolymer PS-Eu-Tb-Zn was synthesized through RAFT polymerization of $Tb(p\text{-}BBA)_3UA$, $Eu(TTA)_2(Phen)MAA$, Zn(BTZ)UA and styrene. The copolymer displays the emission peaks at 421 nm (blue emission), 488, 543 nm (green emission), 589 and 615 nm (red emission) when excited at 365 nm. The CIE coordinates (0.352, 0.330) of the copolymer is highly close to pure white light with the ratio1: 6: 0.45 of complexes **1–3**. The fabricated white LED with the copolymer phosphor shows that the CCT is 5684 K, the CRI (R_a) is 83.1. All the results show that the copolymer is a good candidate as a white component for fabrication of NUV-based white LED.

Acknowledgments

This work was funded by the Program for International Science &Technology Cooperation Program of China (2011DFA52290, 2012DFR50460), Shanxi Provincial Key Innovative Research Team in Science and Technology (2012041011), Natural Science Foundation of Shanxi Province (2013011013-2), and Program for Science and Technology Development of Shanxi (20140321012-01).

References

[1] N. Narendran, M. A. Petruska, M. Achermann, D. J. Webber, E. A. Akhadov, D. D. Koleske, M. A. H. offbauer and V. I. Klimov, *Nano Lett.*, 2005, ***5***, 1039–1044.

[2] E. F. Schubert and J. K. Kim, *Science*, 2005, **308**, 1274–1278.

[3] C. W. Yeh, W. T. Chen, R. S. Liu, S. F. Hu, H. S. Sheu, J. M. Chen and H. T. Hintzen, *J. Am. Chem. Soc.*, 2012, **134**, 14108–14117.

[4] W. L. Wang, Y. H. Lin, W. J. Yang, Z. L. Liu, S. Z Zhiou, H. R. Qian, F. L. Gao, L. Wen and G. Q. Li, *J. Mater. Chem. C*, 2014, **2**, 4112−4116.

[5]W. L. Wang, W. J. Yang, H. Y. Wang and G. Q. Li, *J. Mater. Chem. C*, 2014, **2**, 9342−9358.

[6]W. L. Wang, H. Yang and G. Q. Li, *J. Mater. Chem. C*, 2013, **1**, 4070−4077.

[7]Y. Hu, W. Zhuang, H. Ye, D. Wang, S. Zhang and X. Huang, *J. Alloys Compd.*, 2005, **390**, 226–229.

[8] N. J. Findlay, J. Bruckbauer, A. R. Inigo, B. Breig, S. Arumugam, D. J. Wallis, R. W. Martin and P. J. Skabara, *Adv. Mater.*, 2014, **26**, 7290–7294.

[9] Z. F. Liu, M. F. Wu, S. H. Wang, F. K. Zheng, G. E. Wang, J. Chen, Y. Xiao, A. Q. Wu, G. C. Guo and J. S. Huang, *J. Mater. Chem. C*, 2013, **1**, 4634–4639.

[10] X. G. Huang, G. Zucchi, J. Tran, R. B. Pansu, A. Brosseau, B. Geffroyd and F. Niefa, *New. J. Chem.*, 2014, **38**, 5793–5800.

[11] G. Q. Li, W. L. Wang, W. J. Yang and H. Y. Wang, *Surf. Sci. Rep.*, 2015, **70**, 380−423.

[12] M. M. Shang, C. X. Li and J. Lin, *Chem. Soc. Rev.*, 2014, **43**, 1372−1386.

[13] Y. Liu, J. Hao, W. Zhuang and Y. Hu, *J. Phys. D*, 2009, **42,** 245102/1–245102/6.

[14] L. Li, C. K. Tsung, T. Ming, Z. H. Sun, W. H. Ni, Q. H. Shi, G. D. Stucky and J. F. *Wang*, *Adv. Funct. Mater.*, 2008, **18**, 2956–2962.

[15] D. L. Dexter, *J. Chem. Phys.*, 1953, **21**, 836–840.

[16] W. Zheng, B. B. Wang, J. C. Lai, C. Z. Wan, X. R. Lu, C. H. Li and X. Z. You, *J. Mater. Chem. C*, 2015, **3**, 3072–3080.

[17] A. R. Ramya, M. L. P. Reddy, A. H. Cowley and K. V. Vasudevan, *Inorg. Chem.*, 2010, 49, 2407–2415.

[18] C. Zheng, H. J. Ren, Z. F. Cui, F. H. Chen and G. Y. Hong, *J. Alloys Comp.*, 2009, **477**, 333–336.

[19] I. Nasso, N. Geumc, G. Bechara, B. Mestre-Voegtlé, C. Galaup and C. Picard, *J. Photochem.*

Photobiol. A, 2014, **274**, 124–132.

[20] X. M. Guo, H. D. Guo, L. S. Fu, H. J. Zhang, R. P. Deng, L. N. Sun, J. Feng and S. Dang, *Micropor. Mesopor. Mat.*, 2009, **119**, 252–258.

[21] H. Xu, Q. Sun, Z. F. An, Y. Wei and X. G. Liu, *Coordin. Chem. Rev.*, 2015, **293**, 228–249.

[22] J. Q. Zhang, H. F. Li, P. Chen, W. B. Sun, T. Gao and P. F. Yan, *J. Mater. Chem. C*, 2015, **3**, 1799–1806.

[23] W. T. Xu, Y. F. Zhou, D. C. Huang, M. Y. Su, K. Wang, M. Xiang and M. C. Hong, *J. Mater. Chem. C*, 2015, **3**, 2003–2015.

[24] S. M. Borisov, R. Fischer, R. Saf and I. Klimant, *Adv. Funct. Mater.*, 2014, **24**, 6548–6560.

[25] E. S. Andreiadis, N. Gauthier, D. Imbert, R. Demadrille, J. Pécaut and M. Mazzanti, *Inorg. Chem.*, 2013, 52, 14382–14390.

[26] S. N. A. Jenie, S. Pace, B. Sciacca, R. D. Brooks, S. E. Plush and N. H. Voelcker, *ACS Appl. Mater. Inter.*, 2014, **6**, 12012–12021.

[27] J. B. Yu, L. N. Sun, H. S. Peng and M. I. J. Stich, *J. Mater. Chem.*, 2010, **20**, 6975–6981.

[28]C. Zitzer, T. W. T. Muesmann, J. Christoffers and M. S. Wickleder, *Chem. Asian. J.*, 2015, **10**, 1354–1362.

[29] B. S. Xu, H. X. Xu, X. H. Fang, L. Q. Chen, H. Wang and X. G. Liu, *Org. Electron.*, 2008, **9**, 906–910.

[30] Y. J. Xiong, P. L. Huang, X. W. Zhang, W. Y. Huang, Q. H. Huang, Q. Cheng, J. F. Fang, Y. Li, F. F. Zhu and S. T. Yue, *Inorg. Chem. Commun.*, 2015, **56**, 53–57.

[31] H. G. Yan, H. H. Wang, P. He, J. X. Shi and M. L. Gong, *Synthetic Met.*, 2011, **161**, 748–752.

[32]C. Jangu, J. H. H. Wang, D. Wang, G Fahs, J. R. Heflin, R. B. Moore, R. H. Colby and T. E. Long, *J. Mater. Chem. C*, 2015, **3**, 3891–3901.

[33]E. Frick, A. Anastasaki, D. M. Haddleton and C. Barner-Kowollik, *J. Am. Chem. Soc.*, 2015,**137**, 6889–6896.

[34] H. Mori, M. Matsuyama, K. Sutoh and T. Endo, *Macromolecules*, 2006, **39**, 4351–4360.

[35]L. Z. Borg, A. L. Domanski, A. Breivogel, M. Bürger, R. Berger, K. Heinze and R. Zentel, *J. Mater. Chem. C*, 2013, **1**, 1223–1230.

[36] H. Mori and T. Endo, *Macromol. Rapid Commun.*, 2012, **33**, 1090–1107.

[37] A. Q. Zhang, J. L. Zhang, Q. L. Pan, S. H. Wang, H. S. Jia and B. S. Xu, *J. Lumin.*, 2012,

132 , 965–971.

[38] P. Singh, A. Srivastava and R. Kumar, *Polymer*, 2015, **5**7, 51–61.

[39]M. Crippa, A. Bianchi, D. Cristofori, M. D'Arienzo, F. Merletti, F. Morazzoni, R. Scottia and R. Simonuttia, *J. Mater. Chem. C*, 2013, **1**, 484–492.

[40] A. Q. Zhang, X. D. Hao, J. L. Zhang, H. S. Jia, X. G. Liu and B. S. Xu, *Opt. Mater.*, 2014, **37**, 5–10.

[41] G. L. Zhong and K. Z. Yang, *Langmuir*, 1998, **14**, 5502–5506.

[42] H. X. Xu, B. S. Xu, X. H. Fang, L. Q. Chen, H. Wang and Y. Y. Hao, *J. Photoch. Photobio. A*, 2011, **217**, 108–116.

[43] C. J. Xu, J. T. Wan and B. G. Li, *Dyes Pigments*, 2013, **98**, 493–498.

[44] N. Du, R. Tian, J. Peng and M. Lu, *J. Polym. Sci. Pol. Chem.*, 2005, **43**, 397–406.

[45]X. H. Zhang, R. J. Wei, Y. Y. Zhang, B. Y. Du and Z. Q. Fan, *Macromolecules*, 2015, **48**, 536–544.

[46] Y. Gu, L. P. Zhu, Y. F. Li, L. Yu, K. L. Wu, T. H. Chen, M. L. Huang, F. Wang, S. L. Gong, D. G. Ma, J. G. Qin and C. L. Yang, *Chem. Eur. J.*, 2015, **21**, 8250–8256.

[47]H. H. Wang, P. He, H. G. Yan and M. L. Gong, *Sensor. Actuat. B-Chem.*, 2011, **156**, 6–11.

[48]A. Fischer, T. Koprucki, K. Gartner, M. L. Tietze, J. Bruckner, B. Lussem, K. Leo, A. Glitzky and R. Scholz, *Adv. Funct. Mater.*, 2014, **24**, 3367–3374.

[49] K. Binnemans, *Chem. Rev.*, 2009, **109**, 4283–4374.

[50] V. Divya and M. L. P. Reddy, *J. Mater. Chem. C*, 2013, **1**, 160–170.

[51] S. Sivakumar and M. L. P. Reddy, *J. Mater. Chem.*, 2012, **22**, 10852–10859.

[52] A. R. Ramya , S. Varughese and M. L. P. Reddy, *Dalton Trans.*, 2014, **43**, 10940–10946.

[53] M. Fernandes, V. de Zea Bermudez, R. A. SaFerreira, L. D. Carlos, A. Charas, J. Morgado, M. M. Silva and M. J. Smith, *Chem. Mater.*, 2007, **19**, 3892–3901.

[54] Q. D. Liu, R. Wang and S. Wang, *Dalton Trans.*, 2004, 2073–2079.

[55] C. Seward, J. Pang and S. Wang, *Eur. J. Inorg. Chem.*, 2002, 1390–1399.

[56] T. Forster, *Discuss. Faraday Soc.*, 1959, **27**, 7–17.

[57] T. F. Guo, T. C. Wen, Y. S. Huang, M. W. Lin, C. C. Tsou and C. T. Chung, *Opt. Express*, 2009, **17**, 21205–21215.

[58] J. Q. Zhang, H. F. Li, P. Chen, W. B. Sun, T. Gao and P. F. Yan, *J. Mater. Chem. C*, 2015, **3**,

1799−1806.

[59] G. N. He, D. M. Niedzwiedzki, G. S. Orf, H. Zhang, R. E. Blankenship, *J. Phys. Chem. B*, 2015, **119**, 8321−8329.

[60] L. Li, H. M. Noh, X. G. Liu, B. K. Moon, B. C. Choi, J. H. Jeong, *J. Nanosci. Nanotechno.*, 2015, **15**, 5052−5056.

[61] M. L. Bhaumik and C. L. Telk, *J. Opt. Soc. Am.*, 1964, **54**, 1211−1214.

[62] Z. G. Xia, J. Zhou and Z. Y. Mao, *J. Mater. Chem. C*, 2013, **1**, 5917−5924.

[63] D. G Deng, H. Yu, Y. Q. Li, Y. J. Hua, G. H. Jia, S. L. Zhao, H. P. Wang, L. H. Huang, Y. Y. Li, C. X. Lia and S. Q. Xu, *J. Mater. Chem. C*, 2013, **1**, 3194−3199.